Magnetic anisotropy in epitaxial CrO_2 and CrO_2/Cr_2O_3 bilayer thin films

N. A. Frey, S. Srinath, and H. Srikanth*
Department of Physics, University of South Florida, Tampa, Florida 33620, USA

M. Varela and S. Pennycook
Oak Ridge National Laboratory, Oak Ridge, Tennessee 37831, USA

G. X. Miao and A. Gupta
MINT Center, University of Alabama, Tuscaloosa, Alabama 35487, USA
(Received 7 January 2006; revised manuscript received 22 May 2006; published 21 July 2006)

We have investigated the effective magnetic anisotropy in CVD-grown epitaxial CrO_2 thin films and Cr_2O_3/CrO_2 bilayers using resonant radio-frequency transverse susceptibility (TS). While CrO_2 is a highly spin polarized ferromagnet, Cr_2O_3 is known to exhibit magnetoelectric effect and orders antiferromagnetically just above room temperature. In CrO_2, the measured values for the room temperature anisotropy constant scaled with the film thickness and the TS data is influenced by magnetoelastic contributions at low temperature due to interfacial strain caused by lattice mismatch with the substrate. In CrO_2/Cr_2O_3 bilayers *M-H* loops indicated an enhanced coercivity without appreciable loop shift and the transverse susceptibility revealed features associated with both the ferromagnetic and antiferromagnetic phases. In addition, a considerable broadening of the anisotropy fields and large K_{eff} values were observed depending on the fraction of Cr_2O_3 present. This anomalous behavior, observed for the first time, cannot be accounted for by the variable thickness of CrO_2 alone and is indicative of possible exchange coupling between CrO_2 and Cr_2O_3 phases that significantly affects the effective magnetic anisotropy.

DOI: 10.1103/PhysRevB.74.024420 PACS number(s): 75.30.Gw, 75.70.−i, 75.70.Cn, 77.80.Fm

I. INTRODUCTION

Exchange bias (EB) is a shift of the hysteresis loop along the field axis which occurs when a ferromagnetic (FM) film is in contact with an antiferromagnetic (AFM) film.[1] The shift occurs when the AFM is ordered in the presence of a field or an already ordered FM film. EB in thin films has technological applications in devices such as magnetoresistive sensors.[2] Even though the phenomenon was discovered almost 50 years ago, its microscopic origin is not completely understood. The shift in the hysteresis loop (H_E) is also accompanied by an increase in the hysteresis loop width enhancing the coercivity (H_C). The increase in H_C is observed in many systems[3] and found to be dependent on the thickness of FM and AFM layers.[4] It is believed that both the exchange bias and H_C are the results of interfacial exchange coupling of the AFM and FM layers. In general H_E is observed when the AFM anisotropy is large and for small AFM anisotropy only an enhancement of H_C is observed.[5] Both the effects are observed simultaneously due to the variation of AFM anisotropy by structural defects or grain size distribution. In this paper we present the influence of exchange coupling between the ferromagnetic CrO_2 and antiferromagnetic Cr_2O_3 with varying FM and AFM layer thickness.

Cr_2O_3 is antiferromagnetic with a Néel temperature of 307 K. In zero magnetic field, the Cr^{3+} ions are antiferromagnetically aligned parallel to the rhombohedral *c* axis. When an external magnetic field is applied along the *c* axis, a spin-flop transition occurs above a critical field with the spins switching to lie on the basal plane.[6] Rado *et al.*[7] were the first to experimentally study the existence of both magnetic and electric field-dependent magnetoelectric (ME) effect in Cr_2O_3 powders, and their experiments also unequivocally revealed the existence of antiferromagnetic domains. Domain formation in Cr_2O_3 as the system is cooled below the antiferromagnetic transition has been widely studied. In a recent paper, Borisov *et al.*[8] report the influence of these domains on the exchange bias effect in $Cr_2O_3/(Co/Pt)_3$ that reveals some switching behavior. The electric-field induced magnetization (ME_E) is ascribed due to the distortion in the lattice that breaks the compensation between the two sublattice magnetizations of the antiferromagnet and results in a weak net magnetization.

Another chromium oxide phase, viz. CrO_2 belongs to an important class of magnetic oxides.[9] It is a half-metallic ferromagnet (FM) with a Curie temperature (T_C) of 395 K. Band structure calculations predict a nearly 100% spin polarization (*P*) and this has been confirmed by Andreev reflection and tunneling spectroscopies.[10] The high value of *P* makes it an attractive material for spintronic devices such as magnetic tunnel junctions and spin valves. Combining this material with Cr_2O_3 to form a composite multilayer and studying the overall magnetic response is the motivation of the present work. Dual functionality that combines spintronic and multiferroic properties would be of considerable interest from basic and applied materials perspectives.

To our knowledge, there are not too many investigations of all-oxide, layered composite structures in which one of the layers is a known ME material (like Cr_2O_3) and the second is a ferromagnet or ferroelectric material.[11] The recent study of $Cr_2O_3/(Co/Pt)_3$ and the striking exchange bias effects observed underscore the need for more studies on Cr_2O_3-based sandwich junctions. The characterization of native oxide Cr_2O_3 surface layer on CrO_2 films by Cheng *et al.*[12] revealed

that CrO_2 might polarize the Cr_2O_3 layer. The native Cr_2O_3 surface layer acts as a tunnel barrier and is useful for applications with desirable magneto-transport properties.[13] This prompted us to undertake a systematic investigation of magnetism in Cr_2O_3/CrO_2 bilayers.

In this paper, we present *M-H* characteristics and radio-frequency (RF) transverse susceptibility (χ_T) results that directly probe the change in effective magnetic anisotropy in Cr_2O_3/CrO_2 bilayers. An anomalous trend is observed for varying thickness of Cr_2O_3 that we believe is likely associated with the interface coupling and ME effect in these materials.

II. EXPERIMENTAL

A. Growth of Cr_2O_3/CrO_2 bilayers

High quality epitaxial CrO_2 films were grown on (100)-oriented TiO_2 substrates using an atmospheric pressure chemical vapor deposition (CVD) technique with chromium trioxide (CrO_3) as a precursor, as has been reported previously.[14] In brief, oxygen is used as a carrier gas in a two-zone furnace to transport the precursor from the source region to the reaction zone where it decomposes selectively on the substrate to form CrO_2. The films are grown at a substrate temperature of about 400 °C, with the source temperature maintained at 260 °C, and an oxygen flow rate of 100 sccm. We have studied the transport and magnetic properties of CrO_2 in detail and the results have been reported in several presentations.[13–16]

It is commonly recognized that formation of a natural Cr_2O_3 layer will occur on the CrO_2 surface because it is thermodynamically a much more stable phase than CrO_2.[11,12,16] Because of its metastability, bulk CrO_2 will also irreversibly be reduced to antiferromagnetic Cr_2O_3 at temperatures much higher than about 425 °C. We have taken advantage of this transformation to grow CrO_2/Cr_2O_3 heterostructures of varying relative thickness. For example, by post-annealing a CrO_2 film at 450 °C for varying lengths of time, the film starting from the top surface layer can be controllably converted to Cr_2O_3. All films studied were grown on TiO_2 single crystal (100) substrates with 5×5 mm^2 dimension and of varying thicknesses and Cr_2O_3 content. In order to decouple the effect of thickness on magnetic anisotropy from that of interface coupling in bilayers, we have grown CrO_2 films with varying thickness in the range of 20 nm to 725 nm whereas the total thickness of all the bilayers of CrO_2/Cr_2O_3 was kept constant at 200 nm (except for the variation in volume arising due to the density variation of CrO_2 and Cr_2O_3) with different proportions of CrO_2 and Cr_2O_3.

The CrO_2 and CrO_2/Cr_2O_3 bilayer films were studied using x-ray diffraction (Philips X'Pert) and electron microscopy. Electron microscopy observations were carried out in an aberration corrected scanning transmission electron microscope (STEM) VG Microscopes HB501UX operated at 100 kV. Specimens for STEM were prepared by conventional methods, grinding, dimpling and Ar ion milling.

Figure 1 shows a high resolution cross-sectional *Z*-contrast image of a CrO_2/Cr_2O_3 bilayer film formed by partial thermal decomposition of CrO_2 as discussed above. The two layers are well aligned and form an abrupt interface. The Cr_2O_3 layer is crystalline and it grows coherently on top of the CrO_2 with very few defects. Occasional defects, such as the grain boundary marked by an arrow, propagate directly from the CrO_2 layer. Although we have not studied in detail the epitaxial relationship between the CrO_2 and Cr_2O_3 layers, the x-ray and STEM results suggest that the (0001) plane of the Cr_2O_3 with a corundum structure is parallel to the (100) plane of rutile CrO_2. Further, the in-plane [010] and [001] directions of CrO_2 are aligned with the $[11\bar{2}0]$ and $[\bar{1}100]$ directions of Cr_2O_3, respectively. This epitaxial relationship is consistent with what has been observed for the naturally formed Cr_2O_3 surface layer on commercial acicular CrO_2 particles.[17]

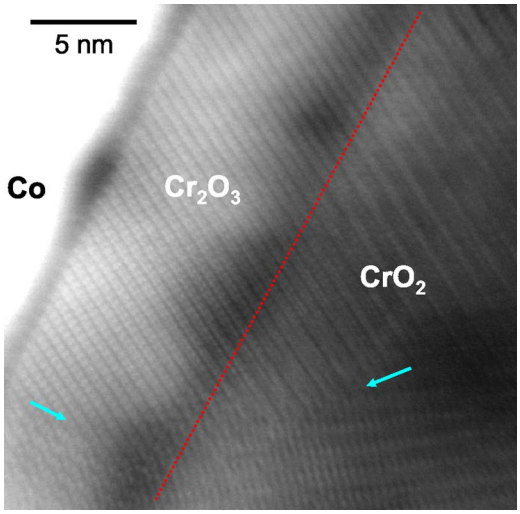

FIG. 1. (Color online) Cross-section high resolution STEM micrograph of heteroepitaxial Cr_2O_3 formed by thermal conversion of CrO_2. A Co layer was deposited on top of Cr_2O_3 to fabricate a tunnel junction structure. A grain boundary defect that propagates across the CrO_2/Cr_2O_3 interface is marked by arrows.

B. Magnetic characterization

The static magnetic properties of the films were studied using an alternating gradient magnetometer (AGM) and a physical property measurement system (PPMS). Figures 2(a) and 2(b) show the magnetization versus applied magnetic field (*M-H*) curves for the CrO_2 films of 21.5 nm and 725 nm thickness, respectively, and Fig. 2(c) shows the *M-H* curves for the 200 nm CrO_2 film (inset) along with the CrO_2/Cr_2O_3 bilayer films with varying content of CrO_2. The step observed in the hysteresis loops near the saturation field in Fig. 2(b) is an artifact of the AGM measurement. As reported earlier for the CrO_2 films, the magnetic easy axis at room temperature changes orientation with thickness.[16] The *M-H* curves at room temperature for the 200 nm and 725 nm show an easy axis for films along the [001] direction and a hard axis along the [010] direction. For the 21.5 nm film, the *M-H* data indicate an easy axis along the [010] direction and a hard axis along the [001] direction. The decrease in saturation magnetization for the bilayer films is due to the de-

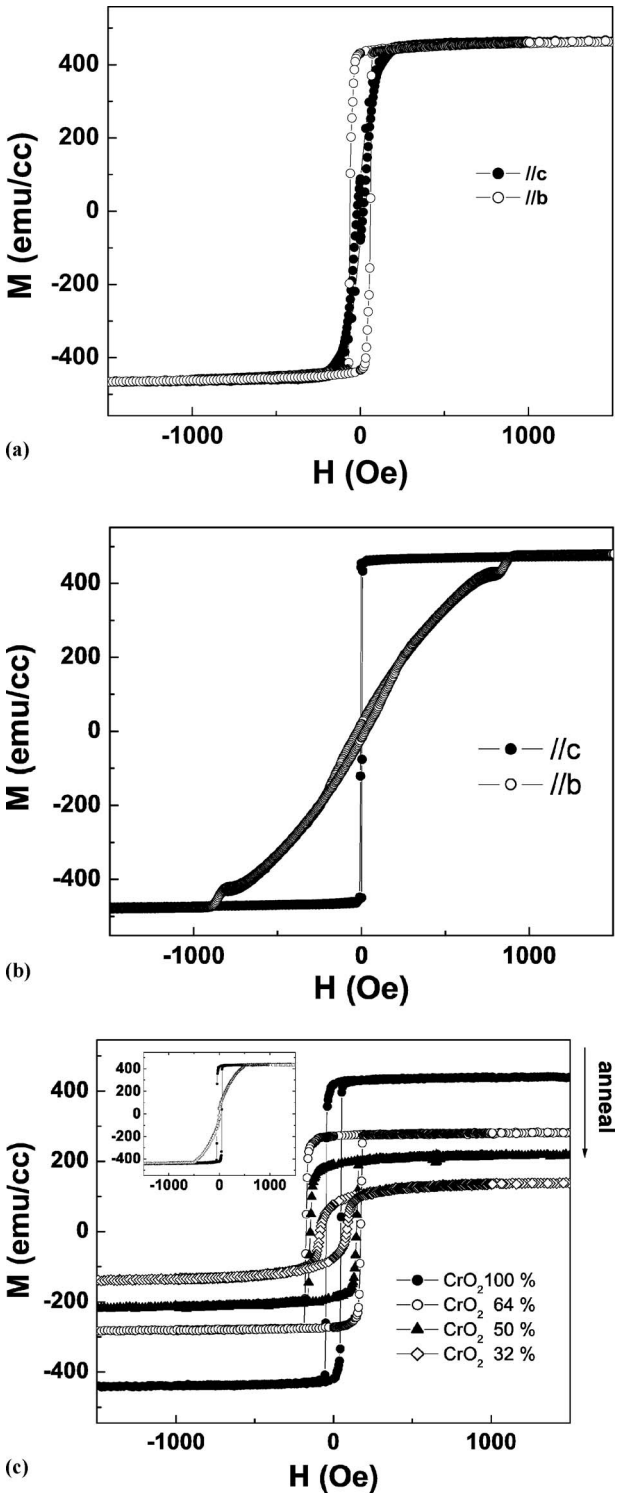

FIG. 2. Hysteresis loops of CrO_2 films and CrO_2/Cr_2O_3 bilayers. (a) 21.5 nm thick CrO_2 film; (b) 725 nm thick CrO_2 film; (c) 200 nm films of varying CrO_2 content after thermal decomposition into CrO_2/Cr_2O_3 bilayers. The inset is for the pure CrO_2 film with 200 nm thickness.

crease in ferromagnetic content (CrO_2) by annealing and conversion to antiferromagnetic Cr_2O_3. The thickness of the Cr_2O_3 layers was deduced from the decrease in saturation magnetization of the bilayer in comparison to the pure CrO_2 film as the Cr_2O_3 contribution is negligible. The estimated percent content of CrO_2 remaining in different bilayer films measured were 64%, 50%, and 32%. Figure 3(a) shows the normalized magnetization of bilayer films as a function of anneal time at 450 °C. The annealing time for the 64%, 50%, and 32% bilayer films are 14 h, 24 h, and 34 h, respectively. For all the bilayers, the room temperature *M-H* curves show a magnetic easy axis along the [001] (*c* axis) and a hard axis along the [010] (*b* axis). In Fig. 3(b) the temperature dependence of the coercivity with variation of CrO_2 content in CrO_2/Cr_2O_3 bilayers is compared with the pure CrO_2 film of the same total thickness of 200 nm. H_C of the bilayer increases in comparison to the pure CrO_2 film depending on the thickness of Cr_2O_3. For the bilayer with 64% of CrO_2 content (~64 nm AFM thickness) enhancement in H_C persists even above the Néel temperature (307 K) up to 350 K. Increase in H_C above T_N is reported in single crystalline exchange biased antiferromagnetic FeF_2 films with Co or Fe (FM) layers.[18,19] This is interpreted due to the short range order induced in the AFM by the ferromagnet. As the CrO_2 (Cr_2O_3) content in the bilayer decreases (increases) the

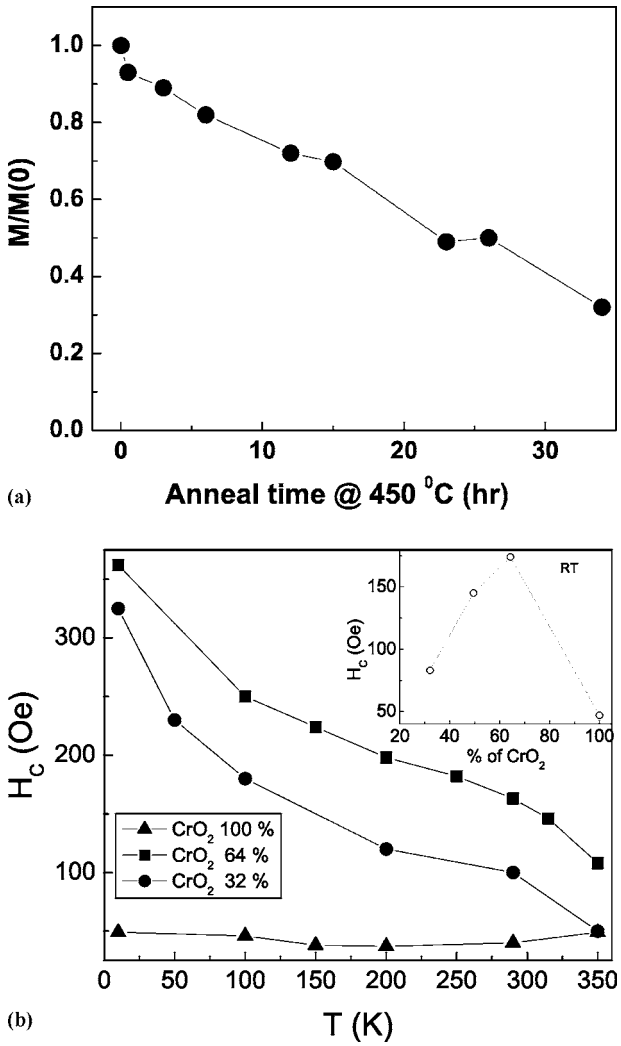

FIG. 3. (a) Normalized magnetization of CrO_2 film as a function of anneal time at 450°; (b) variation of coercivity as a function of % CrO_2 in CrO_2/Cr_2O_3 bilayer film.

variation in H_C decreases and above the Néel temperature it becomes equal to that of pure CrO_2 film. The inset of Fig. 3(b) shows the variation of H_C with CrO_2 content at room temperature. H_C increases from 47 Oe for the 100% CrO_2 film of 200 nm to 174 Oe for the bilayer film with 64% CrO_2 and with further decrease in CrO_2 content H_C decreases. The films with 50% and 32% content CrO_2 have a H_C of 145 Oe and 83 Oe, respectively. H_C for the CrO_2 films alone is inversely proportional to the film thickness whereas for the bilayers, H_C is directly proportional to the FM thickness (t_{FM}). The enhancement and functional dependence of H_C on t_{FM} thickness in the bilayer films strongly suggests the existence of a coupling between the CrO_2 and Cr_2O_3 layers in the bilayer films. To probe the nature of the coupling, we measured the hysteresis loop (not shown) of the bilayer samples by cooling it from above the Néel temperature in a field of 1 Tesla in the same manner as discussed in Ref. 5. We did not see any shift in hysteresis even at $T=10$ K except for the film with the minimum CrO_2 content of 32% (64 nm thickness) for which a small exchange field (H_E) of 12 Oe is observed, indicating that the exchange coupling mechanism in this system is primarily manifested in the enhancement of H_C and not accompanied by H_E.

The role of thickness of the AFM and FM layers in a number of exchange bias systems has been studied in detail. In general either the FM layer or AFM layer thickness is only varied and the main result of these studies indicates that the exchange bias (H_E) and coercivity (H_C) are inversely proportional to the thickness of the FM layer.[3] Furthermore, H_E and H_C are independent of AFM layer thickness (t_{AFM}) for thick films and H_E abruptly decreases and goes to zero for thin t_{AFM}.[3] In our system, the functional dependence of H_E, H_C on t_{FM}, t_{AFM} is rather complicated as both t_{FM} and t_{AFM} are varying in this system. It is the total thickness (200 nm) of the bilayer which is held constant. Apart from this the t_{FM} falls in the range of CrO_2 film thickness wherein both the inhomogeneous strain and the magnetocrystalline anisotropy compete and the easy axis of magnetization switches with both thickness and also temperature. This point will be further discussed in the following sections.

C. Transverse susceptibility as a probe of magnetic anisotropy

RF transverse susceptibility (TS) is known to be an excellent direct method for probing the dynamic magnetization and in particular the effective anisotropy with the external field applied in different orientations with respect to the sample. Over the years, we have successfully applied the TS method to study a wide range of magnetic materials of different forms such as thin films, nanoparticles, and single crystals.[15,20–22]

The experimental technique is based on a sensitive, self-resonant tunnel-diode oscillator (TDO).[23] In this technique a small fixed amplitude (<10 Oe) perturbing RF (12 MHz) field is generated in a coil either parallel or perpendicular to the variable external dc field (H_{dc}) and the relative change in the parallel and transverse components of susceptibility are measured independently. Since the sample is placed in an inductive RF coil that is part of a self-resonant circuit, the shift in the resonant frequency with varying dc field and/or temperature gives a direct measure of the change in inductance and thus the sample susceptibility. Aharoni[24] proposed the first theoretical model of TS based on the Stoner-Wohlfarth formalism. The transverse susceptibility in a unipolar field scan from positive to negative saturation reveals three singularities of which two occur at the anisotropy fields ($\pm H_k$) and one at the switching field. However, in most experimental studies two symmetrical peaks located at the anisotropy fields are easily seen while the third peak is either broadened or merged with one of the peaks due to distribution in grain size and/or close proximity of the switching and anisotropy fields. We will show in this paper that as the temperature is lowered, the change in interfacial strain and the associated magnetoelastic contribution effectively splits the merged peaks and helps in resolving all three peaks in the TS data. TS experiments were done on films of CrO_2 with varying thickness (21 nm, 200 nm, 725 nm) and on bilayers of CrO_2/Cr_2O_3 grown by annealing 200 nm CrO_2 films for different times. The TS curves were measured over a broad range in temperature ($10\ \text{K} < T < 300\ \text{K}$), accessible in a commercial physical property measurement system from Quantum Design, and by applying the external field either along the *b* or *c* axes.

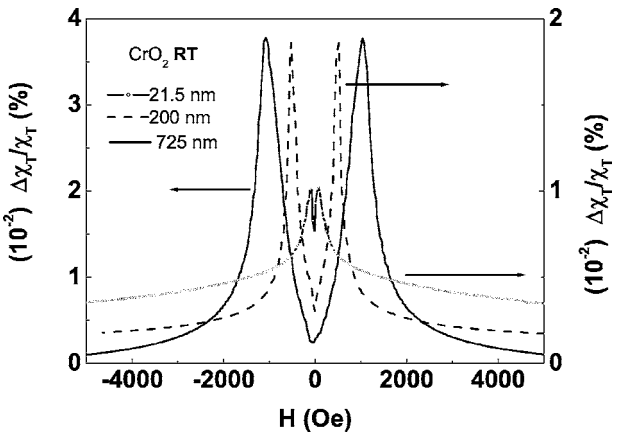

FIG. 4. Transverse susceptibility data with static field applied perpendicular to the easy axis (easy axis for 21.5 nm is [010], for 200 nm and 725 nm [001]) of CrO_2 films of varying thickness at room temperature. The data for the 21.5 nm film is scaled by a factor of 2 for clarity.

III. RESULTS AND DISCUSSION

A. TS measurements on CrO_2 films

Figure 4 shows the field-dependent change in transverse susceptibility $[\Delta\chi_T/\chi_T(\%) \equiv \chi_T]$ obtained for the CrO_2 films with different thicknesses at room temperature with the static magnetic field *H* applied perpendicular to the easy axis (*b* for 21.5 nm and *c* in the case of 200 nm and 725 nm films) of magnetization. Identical peaks are seen in χ_T, symmetrically located around $H=0$, followed by an approach to saturation at higher fields. The fields at which the singular peaks in χ_T are observed are identified as the effective magnetic anisotropy fields (H_k). The peak height increases with increase in

TABLE I. Saturation magnetization, anisotropy field, and anisotropy constants for CrO_2 films at room temperature (RT) and low temperature (LT).

CrO_2 thickness (nm)	M_s (emu/cc) (RT)	H_k (Oe) (RT)	K_{eff} (erg/cc) (RT)	M_s (emu/cc) (LT) Ref. 18	H_k (Oe) (LT)	K_{eff} (erg/cc) (LT)
21.5	465	80	1.9×10^4	640	815	2.6×10^5
200	436	514	1.1×10^5	640	390	1.2×10^5
725	486	1050	2.6×10^5	640	1340	4.3×10^5

film thickness. An increase in anisotropy field H_k with increase in film thicknesses is observed. The positions of these peaks along with the values of saturation magnetization extracted from the M-H curves allow for calculation of the effective anisotropy constant K_{eff} at room temperature using the standard relation $H_k=2M_s/K$. For the 21.5 nm CrO_2 film M_s and H_k are 465 emu/cc and 80 Oe, respectively, yielding a K_{eff} value of 1.9×10^4 erg/cc. The value of H_k increases to 514 Oe for 200 nm and 1050 Oe for the 725 nm films, leading to the effective anisotropy of 1.1×10^5 and 2.5×10^5 erg/cc, respectively. These K_{eff} values extracted from our RF susceptibility data agree well with values of K_{eff} reported by Miao *et al.*[16] from dc magnetic measurements. Room temperature χ_T results along with low temperature values of H_k and K_{eff} are presented in Table I.

The TS measurements for the case when the field is applied parallel to the easy axis show only a single peak consistent with soft ferromagnetic loops seen in the M-H measurements with sharp switching characteristics at very low fields. This aspect of TS dependence on the field orientation is used to probe the temperature dependence of easy axis of magnetization in these films. Temperature dependent TS measurements were done on all three CrO_2 films of different thicknesses in the temperature range of 10 K–300 K. For the 21.5 nm and 725 nm films, the peak in χ_T shifts to higher fields as the temperature decreases and at 10 K the anisotropy fields are close to 815 Oe and 1340 Oe, respectively, and the effective anisotropy values are 2.6×10^5 erg/cc and 4.3×10^5 erg/cc. Figure 5 shows the temperature dependence of H_k for all three films studied. For the 21.5 nm and 725 nm films, a decrease in H_k with increase in temperature is apparent. The temperature variation is dominated by substrate strain effects which introduces a magnetoelastic term to the effective anisotropy. We believe that this data is the first systematic comparison of thickness (strain) effects on the film anisotropy through direct measurements of anisotropy fields over a broad range in temperature.

The 200 nm film shows a slight increase in H_k with increase in temperature. At first glance, this looks counterintuitive but the decrease in anisotropy field with decrease in temperature can be understood in light of a recent paper[16] wherein we had reported that the temperature dependence of competing influence of magnetocrystalline and inhomogeneous strain anisotropy induces a change in easy axis of magnetization for the films in the thickness range of 50–250 nm. The present TS measurements on 200 nm CrO_2 films do seem to display a temperature dependent switching of easy axis of magnetization due to the inhomogeneous strain distribution resulting in a decrease in anisotropy field at lower temperature. The evidence for the inhomogeneous strain distribution in these films from the x-ray rocking measurements of different thickness CrO_2 films is discussed in our previous paper.[16] The main results of the paper are the thinnest film (25 nm) (which is heavily strained) exhibits a sharp peak with a full width at half-maximum (FWHM) of 0.034°. A broader component develops with increase in thickness until it completely dominates, resulting a FWHM of 0.064° for the 310 nm. The two components are clearly noticeable for the intermediate thickness films where double switching is observed. The double switching in these CrO_2 films was also confirmed from the TS measurements on the 200 nm film when the bias H field is applied along the [001] direction at room temperature. No anisotropy peaks are observed indicating that the [001] axis is the easy axis of magnetization. However, when the temperature is lowered, anisotropy peaks start to appear, which would be consistent with a hard axis of magnetization (Fig. 6). As expected, 21.5 nm and 725 nm films when measured in this geometry do not show any anisotropy peaks even at the lowest temperature indicating the absence of magnetization switching.

The variation of H_k as a function of temperature has different slopes for films of different thickness (Fig. 5). However, the effective anisotropy for all the films increases as the temperature is decreased and this is in agreement with the temperature dependence of bulk single crystals.[25] In thin films the strain anisotropy plays a major role and it depends

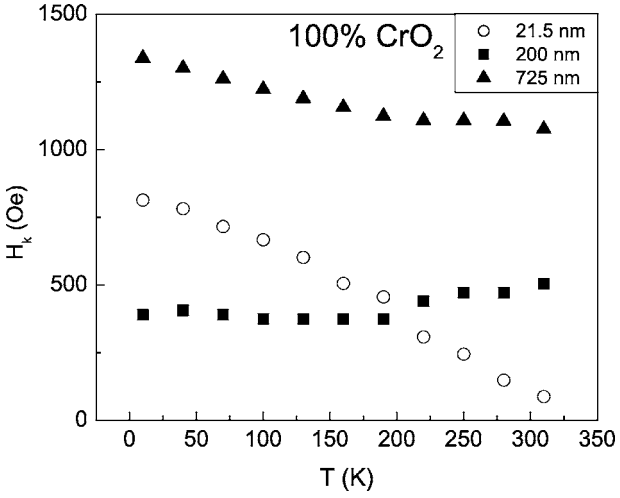

FIG. 5. Temperature dependence of H_k for various thicknesses of CrO_2.

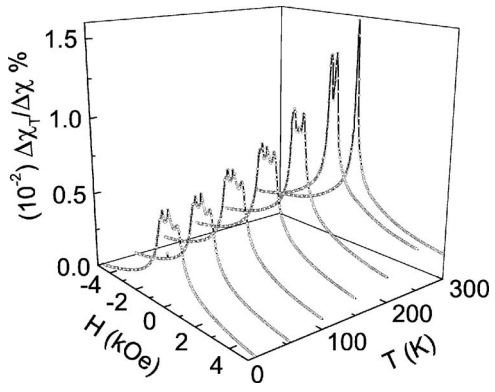

FIG. 6. TS data for 200 nm CrO_2 film taken at different temperatures by applying the static magnetic field along [001], confirming the switching of the magnetic easy axis.

not only on the thickness of the films but also on the temperature. It should be noted that the temperature dependence of H_k is influenced by several effects such as the temperature and anisotropy dependence of the thermal expansion, magnetostriction coefficients and the Young's modulus of the oxide films and the substrate.

B. TS measurements on CrO_2/Cr_2O_3 bilayers

Transverse susceptibility measurements were carried out on all the bilayer samples by applying the static field H parallel to the hard axis [010]. First, TS was measured on a fully decomposed sample to look at the signature due to Cr_2O_3 only. As expected for antiferromagnetic materials, a single sharp peak was present at $H=0$ and the curves did not flatten out at high fields, indicative of the failure to reach saturation. Non saturating magnetization is a known feature in antiferromagnetic materials that is also commonly observed in M -H curves. We also observe a distinct asymmetry in the shape of the TS curves for negative and positive field polarities. This could be associated with slightly different responses of the sublattice magnetization components of the AFM order, when the field is reversed.

The TS measurements on the bilayers interestingly exhibit combined features associated with both the ferromagnetic CrO_2 (anisotropy peaks) and antiferromagnetic Cr_2O_3 (peak at $H=0$) along with the nonsaturation and asymmetry discussed earlier. The TS data for all the samples containing different amounts of CrO_2 percent content at room temperature is presented in Fig. 7. The most noticeable feature of the bilayer data is the shift in the anisotropy peaks to higher fields as the content of Cr_2O_3 increases. The anisotropy peaks are not as sharp as in the case for CrO_2 films but appear as broad shoulders about the center peak. This broadening becomes more pronounced with increase in Cr_2O_3 content until at 32% CrO_2 anisotropy peaks can barely be made out. There is also a prominent strain-associated peak (discussed earlier) that becomes sharper with increase in Cr_2O_3 content.

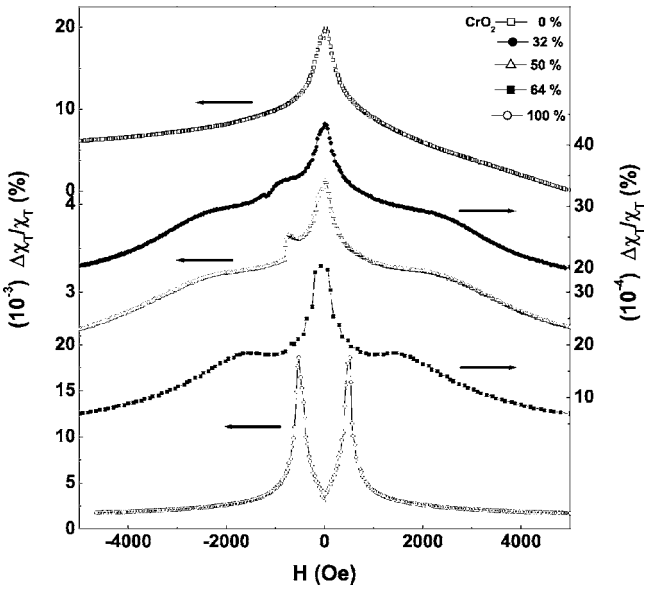

FIG. 7. TS data for CrO_2/Cr_2O_3 bilayer films with varying CrO_2 content.

H_k for the 200 nm 100% CrO_2 film is ~515 Oe whereas for the film with 32% CrO_2 it is ~2100 Oe. The shift in anisotropy peaks to higher fields with decrease in CrO_2 content of the bilayer implies a change in effective anisotropy (K_{eff}). It is important to verify if the increase in H_k corresponds to an increase in K_{eff} after taking into account the corresponding M_S of the t_{FM}. The t_{FM} values based on the percent content of CrO_2 was calculated and is presented in Table II. The corresponding K_{eff} for these thicknesses is obtained by a fit to a curve based on data in Ref. 16. When comparing the observed room temperature K_{eff} values with those calculated based on t_{FM}, it is clear that the observed K_{eff} is consistently larger than what it would be if the Cr_2O_3 were not present in the films. The maximum K_{eff} (2.4

TABLE II. Saturation magnetization, anisotropy field, and anisotropy constants for CrO_2/Cr_2O_3 bilayer films of different Cr_2O_3 content measured at room temperature (RT) and low temperature (LT).

% CrO_2	Effective thickness (nm)	M_s (emu/cc) (RT)	H_k (Oe) TS (RT)	K_{eff} (erg/cc) (observed) (RT)	K_{eff} (erg/cc) (calculated)	H_k (Oe) (cal)	H_k (Oe) TS (LT)	M_s (emu/cc) (LT)	K_{eff} (erg/cc) (LT)
100	200	436	514	1.1×10^5	1.1×10^5	514	390	660	1.3×10^5
64	128	291	1448	2.1×10^5	4.6×10^4	314	2130	423	4.5×10^5
50	99	227	2075	2.3×10^5	6.2×10^4	548	3150	326	5.1×10^5
32	64	136	2100	1.4×10^5	7.7×10^4	1136	3230	212	3.4×10^5

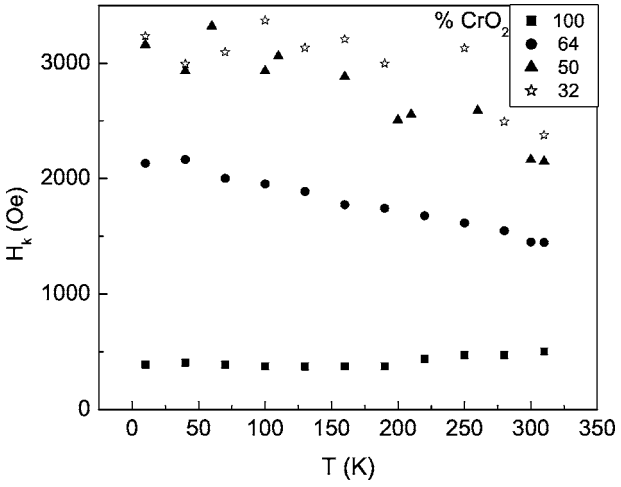

FIG. 8. Temperature dependence of H_k for bilayers with varying CrO_2 content.

$\times 10^5$ erg/cc) was obtained for a bilayer film with 50% content of CrO_2, which is much larger in comparison to the K_{eff} calculated (6.2×10^4 erg/cc). The results for all the films are given in Table II. For the pure CrO_2 films H_k is proportional to CrO_2 thickness (Table I), whereas for the bilayers H_k is inversely proportional to the t_{FM} (Table II). The role of Cr_2O_3 and its interface with CrO_2 is manifested not only by the enhancement of H_k but also by its functional dependence with t_{FM}.

The temperature dependence of H_k for the bilayers is plotted in Fig. 8. For all bilayer films, an increase in H_k with decrease in temperature is observed. This indicates that the presence of Cr_2O_3 changes the temperature dependence of the strain in comparison to the pure CrO_2 films thereby the easy axis of magnetization remains along the c axis throughout the temperature range. This is also evident from the absence of the anisotropy peaks throughout the temperature range when the TS is measured with the applied field parallel to the easy axis. Similar to the room temperature measurements, H_k increases with increase in Cr_2O_3 content throughout the measured temperature range. Low temperature K_{eff} values were calculated from H_k measured at 10 K. While the values of K_{eff} for the CrO_2 thin films matched well with those reported in Ref. 16, the K_{eff} values for the bilayers were consistently larger throughout the temperature range, again indicating coupling between the layers. The nature of coupling can be probed by TS as it is also sensitive to the presence of exchange coupling.[26] The field dependent TS with the static magnetic field applied parallel to the easy axis would show a shifted hysteresis in TS with a single peak if exchange anisotropy (H_E) were present. Our TS measurements on these bilayer samples do not show the shifted hysteresis loops which are consistent with the absence of loop shifting in the M-H curves.

As discussed in the Introduction, an increase in H_C without H_E is observed when the anisotropy of AFM is small but in the case of CrO_2/Cr_2O_3 bilayers the anisotropy of the FM and AFM are of similar magnitude $\sim 2\times 10^5$ erg/cm^3. No exchange bias was observed in the case of as-received commercial CrO_2 particles of $50\times 50\times 200$ nm^3 size enclosed by epitaxial by 2.5 nm thickness Cr_2O_3 layer.[17] To observe the exchange bias based on the random field model using the condition that the anisotropy of the AFM must be larger than the interface coupling energy, i.e., $4z\sqrt{A_{\text{AFM}}K_{\text{AFM}}}/\pi^2 < K_{\text{AFM}}t_{\text{AFM}}$ where A_{AFM} and K_{AFM} are the exchange stiffness and anisotropy constant, the minimum thickness of the AFM layer is calculated to be 5.7 nm.[17] Zheng *et al.*[17] annealed these particle systems in air at 600° for 1 hour and the thickness of the Cr_2O_3 shell is increased thereby the t_{AFM} and t_{FM} were 36 and 3 nm, respectively. In the case of annealed particles the exchange bias of 220 Oe was observed consistent with the theoretical value calculated using $H_E = 2z\sqrt{A_{\text{AFM}}K_{\text{AFM}}}/(\pi^2 M_{\text{FM}}t_{\text{FM}})$. Though the minimum t_{AFM} in our bilayer system is ~64 nm, we do not see any exchange shift which is rather surprising. The observed behavior in this exchange coupled bilayers may be understood in terms of a theoretical model proposed by Schulthess *et al.*[27] According to this model, the spin-flop coupling between the FM/AFM bilayers with perfectly flat interface gives rise to a uniaxial anisotropy (increase in H_C) rather than a unidirectional anisotropy (H_E). The Cr_2O_3/CrO_2 interface exhibits near-perfect epitaxy as observed in high resolution STEM images. Recently Kuch *et al.*[28] based on their study of magnetic interface coupling between AFM/FM films with well-defined single crystalline interfaces report that flat interfaces do not contribute to the exchange coupling and instead modifies the uniaxial antiferromagnetic spin structure.

The total thickness (200 nm) of the bilayer under study falls in the region of CrO_2 thickness which exhibits a double switching phenomenon due to the inhomogeneous strain distribution caused by the substrate. Hence the magnetization of the bilayers is the resultant of the inhomogeneous strain distribution caused by the substrate at one end and the exchange coupling with the AFM Cr_2O_3 at the other end. Another striking feature from these combined analyses of M-H and TS on the bilayer system is the variation of H_C and H_k with t_{FM}. Thus, Cr_2O_3 presence in the bilayer affects the two most important magnetic properties, i.e., switching field (H_C) and the anisotropy fields (H_k) establishing the coupling between the CrO_2 and the Cr_2O_3 layers. It should be noted that the CrO_2/Cr_2O_3 bilayer is a EB system in which the top layer is a ME AFM (Cr_2O_3) layer. Recently[8] magnetoelectic switching of EB is shown in $Cr_2O_3/(Co/Pt)_3$ wherein Co/Pt multilayer is grown on Cr_2O_3 single crystals of 0.7 nm thickness. So apart from EB, ME may also play a role in the observed variation of H_C and H_k. However, a true probe of the ME effect would require investigating M-H loops and TS under applied electric fields. We are currently setting up these experiments which require a fair amount of technical finesse in designing the inserts for PPMS. Our observations of the ME effect under applied voltage bias will be investigated and reported in the future but they are beyond the scope of this paper.

For a complete understanding of the role of the interface, more direct measurements such as polarized neutron reflectivity probing the interface and also study of exchange bias effect in bilayers with a rough interface are required and will be further investigated in our continued study of these bilayers.

IV. CONCLUSIONS

We have grown CrO_2 thin films and CrO_2/Cr_2O_3 bilayers on (100)-TiO_2 substrates by chemical vapor deposition and studied their static and dynamic magnetic properties. Our results indicate that while H_k varies with temperature for most thicknesses of CrO_2 films, for a critical thickness around 200 nm the temperature dependence of H_k is nearly constant. This would imply that films of this thickness could be optimized for uniform properties in devices such as magnetic tunnel junctions that are operational over a broad range in temperature.

The transverse susceptibility measurements on the bilayers exhibited features associated with both the antiferomagnetic and ferromagnetic materials. We also observe an overall increase in H_k and K_{eff} with increase in Cr_2O_3 content. The coupling between the CrO_2 and Cr_2O_3 layers is not only shown by the shift of anisotropy peaks to higher fields as measured by TS but also by the variation of the coercivity (which represents the switching field) with increase in Cr_2O_3 content. Thus, Cr_2O_3 presence in the bilayer effect the two most important magnetic properties i.e., switching field and the anisotropy fields establishing the coupling between the CrO_2 and the Cr_2O_3 layers.

ACKNOWLEDGMENTS

Research at USF was supported by DARPA/ARO through Grant No. W911NF-05-1-0354. Research at Alabama was supported by NSF MRSEC Grant No. DMR-0213985. Research at ORNL was sponsored by the Laboratory Directed Research and Development Program of ORNL, managed by UT-Batelle, LLC, for the U.S. Department of Energy under Contract No. DE-AC05-00OR22725.

*Corresponding author. Electronic address: sharihar@cas.usf.edu

[1] W. H. Meiklejohn and C. P. Bean, Phys. Rev. **102**, 1413 (1956).
[2] S. S. P. Parkin, K. P. Roche, M. G. Samant, P. M. Rice, R. B. Beyers, R. E. Scheuerlein, E. J. O'Sullivan, S. L. Brown, J. Bucchigano, D. W. Abraham, Yu Lu, M. Rooks, P. L. Trouilloud, R. A. Wanner, and W. J. Gallagher, J. Appl. Phys. **85**, 5828 (1999).
[3] J. Nogués and I. K. Schuller, J. Magn. Magn. Mater. **192**, 203 (1999); A. E. Berkowitz and K. Takano, *ibid.* **200**, 552 (1999).
[4] R. Jungblut, R. Coehoorn, M. T. Johnson, J. Aan de Steege, and A. Reinders, J. Appl. Phys. **75**, 6659 (1994); C. Leighton, M. R. Fitzsimmons, A. Hoffmann, J. Dura, C. F. Majkrzak, M. S. Lund, and I. K. Schuller, Phys. Rev. B **65**, 064403 (2003).
[5] J. Nogués, J. Sort, V. Langlais, V. Skumryev, S. Suricach, J. S. Mucoz, and M. D. Bary, Phys. Rep. **422**, 65 (2005).
[6] M. Muto, Y. Tanabe, T. Iizuka-Sakano, and E. Hanamura, Phys. Rev. B **57**, 9586 (1998).
[7] G. T. Rado and V. J. Flen, Phys. Rev. Lett. **7**, 310 (1961).
[8] P. Borisov, A. Hochstrat, X. Chen, W. Kleemann, and C. Binek, Phys. Rev. Lett. **94**, 117203 (2005).
[9] A. Gupta and J. Z. Sun, J. Magn. Magn. Mater. **200**, 24 (1999).
[10] J. Soulen, J. M. Byers, M. S. Osofsky, B. Nadgorny, T. Ambrose, S. F. Cheng, P. R. Broussard, C. T. Tanaka, J. Nowak, J. S. Moodera, A. Barry, and J. M. D. Coey, Science **282**, 85 (1998); Y. Ji, G. S. Strijkers, F. Y. Yang, C. L. Chien, J. M. Byers, A. Anguelouch, G. Xiao, and A. Gupta, Phys. Rev. Lett. **86**, 5585 (2001); J. S. Parker, S. M. Watts, P. G. Ivanov, and P. Xiong, *ibid.* **88**, 196601 (2002).
[11] M. Gajek, M. Bibes, A. Barthélémy, K. Bouzenhouane, S. Fusil, M. Varela, J. Fontcuberta, and A. Fert, Phys. Rev. B **72**, 020406(R) (2005).
[12] R. Cheng, C. N. Borca, N. Pilet, B. Xu, L. Yuan, B. Doudin, S. H. Liou, and P. A. Dowben, Appl. Phys. Lett. **81**, 2109 (2002).
[13] A. Gupta, X. W. Li, and G. Xiao, Appl. Phys. Lett. **78**, 1894 (2001).
[14] X. W. Li, A. Gupta, T. R. McGuire, P. R. Duncombe, and G. Xiao, J. Appl. Phys. **85**, 5585 (1999).
[15] L. Spinu, H. Srikanth, A. Gupta, X. W. Li, and G. Xiao, Phys. Rev. B **62**, 8931 (2000).
[16] G. Miao, G. Xiao, and A. Gupta, Phys. Rev. B **71**, 094418 (2005).
[17] R. K. Zheng, H. Liu, Y. Wang, and X. X. Zhang, Appl. Phys. Lett. **84**, 702 (2004).
[18] C. Leighton, H. Schl, M. J. Pechan, R. Compton, J. Nogués, and I. K. Schuller, J. Appl. Phys. **92**, 1483 (2002).
[19] M. Grimsditch, A. Hoffman, P. Vavossori, H. Shi, and D. Lderman, Phys. Rev. Lett. **90**, 257201 (2003).
[20] P. Poddar, J. L. Wilson, H. Srikanth, D. F. Farrell, and S. A. Majetich, Phys. Rev. B **68**, 214409 (2003); R. Swaminathan, M. E. McHenry, P. Poddar, and H. Srikanth, J. Appl. Phys. **97**, 10G104 (2005).
[21] P. Poddar, G. Woods, S. Srinath, and H. Srikanth, IEEE Trans. Nanotechnol. **4**, 59 (2005).
[22] G. T. Woods, P. Poddar, H. Srikanth, and Ya. M. Mukovskii, J. Appl. Phys. **97**, 10C104 (2005).
[23] H. Srikanth, J. Wiggins, and H. Rees, Rev. Sci. Instrum. **70**, 3097 (1999).
[24] A. Aharoni, E. H. Frei, S. Shtrikman, and D. Treves, Bull. Res. Counc. Isr., Sect. F **6A**, 215 (1957).
[25] D. S. Rodbell, J. Phys. Soc. Jpn. **21**, 1224 (1966).
[26] L. Spinu, Al. Stancu, Y. Kubota, G. Ju, and D. Weller, Phys. Rev. B **68**, 220401 (2003).
[27] T. C. Schulthess and W. H. Butler, Phys. Rev. Lett. **81**, 4516 (1998).
[28] W. Kuch, L. I. Chelaru, F. Offi, J. Wang, M. Kotsugi, and J. Kirschner, Nat. Mater. **5**, 128 (2006).